DEPENDENCE OF MUON COLLIDER LUMINOSITY ON IONIZATION COOLING PERFORMANCE*†

M. Vanwelde‡[1], C. Carli[1], D. Schulte[1], B. Stechauner[1], R. Taylor[1]
[1]CERN, Geneva, Switzerland

Abstract

A 10 TeV center-of-mass muon collider is a high-energy lepton collider that has the potential to achieve physics reach comparable to significantly larger hadron colliders. The final luminosity depends on the performance of the entire complex, from muon beam production to the collider ring, including the rapid cooling and acceleration stages. Achieving the target luminosity imposes stringent constraints on the ionization cooling and the collider optics, such as extremely small betatron functions at the interaction points, which induce strong chromatic effects that ultimately limit the machine momentum acceptance. To meet the momentum acceptance requirements without significant luminosity loss, one possible strategy is to end the muon cooling stage earlier, since a reduction of the longitudinal emittance can be traded against larger transverse emittances with a shorter cooling system. A study of a common optimization of the ionization cooling and the collider ring design to maximize the luminosity is presented in this work.

INTRODUCTION

A 10 TeV center-of-mass muon collider is a high-energy lepton collider with the potential to deliver an integrated luminosity of approximately 10 ab^{-1} [1–4] with its nominal parameters, shown in Table 1 [5]. Muon beams, which originate from pion decay, have large transverse and longitudinal emittances, requiring fast ionization cooling due to their short lifetime [6]. The cooling system consists of two main stages. The rectilinear 6D cooling channel reduces both transverse and longitudinal emittances to near-equilibrium values. It is followed by the final cooling channel, which aims to reach the target parameters by further reducing the transverse emittance, at the cost of an increase in longitudinal emittance. The specific design of these cooling channels, along with the underlying assumptions and initial parameters, affects both the transmission and the transverse and longitudinal emittances at the end of the cooling system. Hence, the design and performance of the ionization cooling channel strongly influence the achievable luminosity.

In addition to beam characteristics determined by the cooling channels and fast acceleration, the luminosity also depends strongly on the optics of the collider itself. Specifically, the Twiss betatron functions at the interaction points (IPs) need to be as small as possible. The nominal collider parameters are based on the nominal longitudinal emittance and the assumption that an RMS momentum spread of $1 \cdot 10^{-3}$ is achievable, corresponding to an RMS bunch length of 1.5 mm. Setting $\beta^* = 1.5$ mm to the bunch length allows to keep a reasonable hourglass factor f_{hg}. However, such a small β^* makes the optics very challenging, with very large peak β-functions and strong chromatic aberrations that must be efficiently compensated to meet the dynamic aperture (DA) and momentum acceptance (MA) requirements (typically a DA of 3-4 times the RMS beam size over a momentum range of 2-3 times the RMS momentum spread). The current collider design satisfies these requirements for an imperfection-free machine only when β^* is relaxed from 1.5 mm to 3 mm, at the cost of reduced luminosity [7].

Table 1: Main Nominal Parameters of the 10 TeV Muon Collider Ring

Parameter	Symbol	Value
Beam energy [GeV]	E	5000
Luminosity per IP [10^{34}cm^{-2} s^{-1}]	$\mathscr{L}$	20
Bunch population [10^{12}]	N_p	1.8
Norm. transverse RMS emittance [µm]	$\varepsilon_{n,x} = \varepsilon_{n,y}$	25
Geom. transverse RMS emittance [nm]	$\varepsilon_{g,x} = \varepsilon_{g,y}$	0.528
Longitudinal emittance [mm]	ε_l	71
RMS bunch length [mm]	σ_z	1.5
Relative RMS momentum spread [%]	$\delta = \frac{\sigma_p}{p}$	0.1
Beta function at IP [mm]	$\beta_x^* = \beta_y^*$	1.5
Repetition rate [Hz]	f_r	5

As luminosity depends on all stages of the muon collider complex, a start-to-end simulation and optimization of the entire complex are required [8]. A first step in this overall optimization is to evaluate the impact of the ionization cooling performance on the luminosity. One strategy to increase the available luminosity is to end the muon cooling stage earlier, resulting in a significant reduction of the longitudinal emittance with only moderately larger transverse emittances. Reduced longitudinal emittance can facilitate meeting the MA requirements, potentially enabling a smaller optimized β^*. A shorter cooling system also achieves higher beam intensities, thus increasing the final luminosity, and has implications for hourglass effects and beam-beam strength.

This paper reports on a first common optimization of ionization cooling and collider ring design to maximize luminosity. In particular, this work evaluates the achievable luminosity when stopping the cooling channel at different stages (number of cooling cells). The performance of a specific design of the final cooling based on realistic assumptions is detailed.

* Work endorsed by the IMCC.
† Funded by the European Union (EU). Views and opinions expressed are however those of the author(s) only and do not necessarily reflect those of the EU or European Research Executive Agency (REA). Neither the EU nor the REA can be held responsible for them.
‡ marion.vanwelde@cern.ch

IMPACT OF COOLING EMITTANCE ON β^*

In the presently available designs of the final cooling stage [9, 10], the transverse emittances at the exit of the cooling channel are close to (but slightly above) the target values, while the longitudinal emittance is slightly smaller compared to the target value. This configuration reduces momentum spread and mitigates chromatic effects in the collider ring, although transmission remains below target [8]. The final cooling performance strongly depends on the preceding 6D cooling stage. While different 6D cooling lattices [11–13] achieve similar longitudinal emittance, they vary in transverse emittance and transmission. A longer 6D cooling stage produces lower transverse emittance at the cost of slightly higher decay losses. In contrast, a shorter lattice improves transmission but results in larger transverse emittance. Starting with a smaller transverse emittance into the final cooling stage allows faster convergence to target values and results in a smaller longitudinal emittance, which is beneficial for the subsequent fast acceleration chain.

The final cooling lattice used in this work is an updated version of the current final cooling design [10, 14], and uses beam parameters from the longer 6D cooling channel. Realistic assumptions are implemented, including liquid and gaseous hydrogen absorbers, lithium hydride and silicon nitride beam windows, a 40 T solenoid based on the CERN design [15], and separated solenoid and RF-cavity modules. The lattice consists of nine final-cooling cells, with an average muon loss of about 5% per cell. The achieved emittances after each cooling cell are summarized in Table 2, along with the corresponding emittances and particle numbers in the downstream collider ring. These values include a 10% increase in emittance between the cooling and collider ring, introduced as a design margin for beam degradation along the acceleration chain [12, 16], and assume that the nominal intensity is reached for nine cooling cells. For completeness, two additional cells have been included by extrapolating beyond the lattice to assess performance at target emittances.

Table 2: Cooling performance and collider projections. The last row corresponds to the nominal values and requirements.

#Cell	Cooling		Collider			
	$\varepsilon_{n,t}$[μm]	ε_l[mm]	$\varepsilon_{n,t}$[μm]	ε_l[mm]	β^*[mm]	N[10^{12}]
1	105	1.67	116	1.84	-	2.79
2	86.7	2.60	95.3	2.86	-	2.70
3	75.4	3.72	82.9	4.09	-	2.63
4	58.5	6.58	64.3	7.24	-	2.43
5	45.9	10.9	50.4	12.0	1.85	2.24
6	37.6	17.3	41.4	19.0	1.95	2.21
7	33.3	22.5	36.6	24.8	2.00	2.08
8	30.4	27.5	33.5	30.3	2.10	1.92
9	25.5	42.9	28.0	47.2	2.30	1.80
10	22.7	51.4	25.0	56.5	2.55	1.69
11	18.5	64.5	20.3	71.0	2.80	1.59
Req.	22.7	64.5	25.0	71.0	1.50	1.80

The impact of the ionization cooling channel on collider performance and luminosity has been evaluated based on the latest collider lattice design [7]. Luminosity computations account for the short muon lifetime and the resulting muon decays occurring in the ring during operation [4]:

$$\mathscr{L} = \frac{f_r N^2}{8\pi\, \varepsilon_{g,t}\, \beta^*} f_{\mathrm{hg}}\, \frac{\gamma\, T_\mu}{T_{\mathrm{rev}}}, \tag{1}$$

where f_r is the repetition rate, N is the number of muons in the single muon beam bunch, $\varepsilon_{g,t}$ is the geometric transverse emittance, f_{hg} the hourglass factor, T_μ is the muon lifetime at rest and T_{rev} the revolution time. The transverse emittance directly affects the luminosity and, indirectly, the achievable β^* at the IPs. Specifically, the transverse emittance determines the beam size in the final focusing (FF) quadrupoles, which in turn constrains their aperture and maximum achievable gradient. Larger transverse emittances increase the transverse beam envelopes $\sigma_{x,y}$ and required apertures ($a = 5\sigma + 4$ cm, where $\sigma = \max(\sigma_x, \sigma_y)$, $\sigma_{x,y} = \sqrt{\beta\varepsilon + (D\delta)^2}$, and the additional 4 cm accounts for tungsten shielding against secondary particles from muon decay [7, 17]), which in turn reduces the achievable quadrupole gradients [18]. The longitudinal emittance, on the other hand, affects either the bunch length or the momentum spread in the collider ring. A smaller momentum spread helps meet MA requirements more easily.

To study the impact of the final cooling system length on luminosity, we performed sensitivity studies on the β^* parameter, similar to the one described in [7], using beam parameters from cooling channels with varying numbers of cooling cells, as listed in Table 2. For each case, the FF triplet was adapted to the adjusted transverse emittance by adjusting its length and quadrupole gradients according to their updated apertures, to remain within the magnetic field limits of high-temperature superconducting (HTS) quadrupoles [18]. The lattice was then re-matched for different β^* values, maintaining comparable working points and tune shifts with momentum across all β^* values. The momentum acceptance for given minimum transverse DAs over 100 turns was then computed for all β^*. Figure 1(a) shows the results obtained with beam characteristics expected in the collider ring with six final cooling cells. From this plot, we find that a β^* of 1.95 mm is optimal for six cooling cells, with the DA being three times the RMS beam size within a relative momentum offset interval of $\pm 3\sigma_\delta$. Similarly, the smallest β^* satisfying the DA and MA requirements without magnetic field and positioning errors was identified for different numbers of cooling cells, as indicated in Table 2. The reduced longitudinal emittance at the end of a shorter cooling system leads to less stringent constraints on momentum acceptance, thereby allowing for smaller β^* values. In this study, we also assumed that the bunch length matches β^*, further reducing the momentum spread as β^* increases, as shown by the dashed lines in Fig. 1(a).

IMPACT OF FINAL COOLING LENGTH ON LUMINOSITY

Once the minimum β^* that allow the collider to meet the DA and MA requirements for several cooling cells were

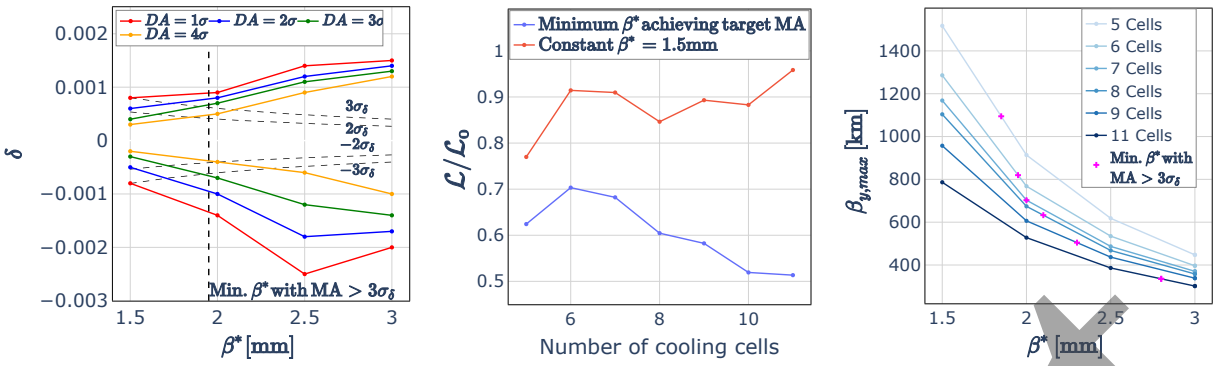

(a) (b) (c)

Figure 1: (a) Momentum acceptance for given transverse DAs as a function of β^* for 6 final cooling cells. (b) Available luminosity and (c) Maximum β_y in the FF triplet as a function of β^*, for varying number of final cooling cells.

determined, we computed the luminosity by accounting for all factors affected by the cooling system length. When assuming a constant β^* of 1.5 mm, the luminosity remains roughly constant along the last cooling cells of the final cooling stage, even slightly increasing for additional cells with reduced transverse emittance. However, when realistic β^* values that include collider constraints are considered, the optimum luminosity is achieved with fewer cooling cells, as shown in Fig. 1(b). A shorter cooling lattice increases luminosity, but the resulting smaller optimized β^* values lead to higher maximum β functions in the FF triplet, which are further enhanced by the reduced FF quadrupole gradients due to larger apertures from increased transverse emittances, as shown in Fig.1(c). This may pose technological challenges for magnet design, as the required apertures approach the limits of current magnet technology, not to mention that the FF quadrupole apertures still need to be increased in future iterations of the collider lattice to account for more realistic assumptions in the IR, such as thicker tungsten shielding for heat load mitigation and longer interconnects between magnets [19]. For the design considered in this study, a good compromise is to use seven cooling cells, resulting in emittances of $\varepsilon_{n,t} = 33.3\,\mu$m and $\varepsilon_l = 22.5$ mm.

These preliminary results indicate that some luminosity can be regained compared to previous studies [7] by slightly reducing the length of the final cooling channel. The luminosity reduction due to increased transverse emittance appears to be largely compensated by the lower achievable β^* and the higher transmission and beam intensities in the collider ring for a shorter cooling system. However, even though this strategy increases the available luminosity, it still does not reach the nominal value of $\sim 20 \cdot 10^{34}\text{cm}^{-2}\,\text{s}^{-1}$ per IP. This study also shows that there is a maximum transverse emittance that can be tolerated in the collider lattice, limited by the resulting increase in the maximum β functions and the corresponding reduction in momentum acceptance. The collider design imposes a limit on trading off a reduction in longitudinal emittance against larger transverse emittances: the final cooling lattice must achieve a sufficiently small transverse emittance (below 50 µm) for this study to remain valid and meaningful.

Finally, no margin has been included when determining the achievable β^* for each cooling cell. These results therefore do not yet account for the fact that the collider lattice will need to be adapted to meet the requirements of combined-function magnets and shielding outside the IR, which may lead to a reduction in overall collider performance and a larger β^*. Other factors also need to be considered in future studies, including the impact of a larger number of muons remaining in the collider when new bunches are injected for higher beam intensities. Further studies on collective effects, e.g. beam-beam interactions, are also required to evaluate their impact on luminosity but also on the overall collider optics and beam dynamics.

CONCLUSION

In this work, a procedure for the joint optimization of the ionization cooling system and the collider ring design to maximize luminosity has been presented. The transverse and longitudinal emittances and the beam intensity in the collider ring depend on the ionization cooling channel. Beam characteristics at the collider corresponding to different numbers of cells in an existing final cooling channel were used to maximize the luminosity. For each case, the collider lattice has been re-matched to different values of β^*, followed by an evaluation of the MA for different minimum DA values. The smallest β^* resulting in a DA of three times the RMS beam size over a relative momentum offset range of $\pm 3\sigma_\delta$ has been retained as optimized value and used to compute the achievable luminosity in all cases. Preliminary results indicate that a shorter final cooling system could enhance the luminosity, although caution is needed because larger transverse emittances impose technological constraints, particularly on the large-aperture FF quadrupoles. Further optimization of the collider and cooling system is still required to reach the target luminosity and include increasingly realistic assumptions. While this study provides initial insights into potential joint optimization of the cooling and collider lattices, a more comprehensive optimization of the entire muon collider complex is required to achieve the maximum luminosity possible.

REFERENCES

[1] D. Stratakis *et al.*, "A muon collider facility for physics discovery", in *Proc. 2021 US Community Study on the Future of Particle Physics (Snowmass'21)*, 2021. doi:10.48550/arXiv.2203.08033

[2] K. R. Long, D. Lucchesi, M. A. Palmer, N. Pastrone, D. Schulte, and V. Shiltsev, "Muon colliders to expand frontiers of particle physics", *Nat. Phys.*, vol. 17, no. 3, pp. 289–292, Mar. 2021. doi:10.1038/s41567-020-01130-x

[3] D. Schulte, "The International Muon Collider Collaboration", in *Proc. 12th Int. Particle Accel. Conf. (IPAC'21)*, Campinas, SP, Brazil, May 2021, pp. 3792–3795. doi:10.18429/JACoW-IPAC2021-THPAB017

[4] C. Accettura *et al.*, "Towards a muon collider", *Eur. Phys. J. C*, vol. 83, no. 9, p. 864, 2023. doi:10.1140/epjc/s10052-023-11889-x

[5] R. Taylor *et al.*, "MuCol Milestone Report No. 5: Preliminary Parameters", in in *MuCol – A Design Study for a Muon Collider Complex at 10+ TeV Center of Mass*, Oct. 2024, doi:10.5281/zenodo.13970100,

[6] D. Neuffer, "Principles and applications of muon cooling", in *Proceedings of the Third LAMPF II Workshop*, vol. 1, Los Alamos, NM, USA, p. 470, Jul. 1983.

[7] M. Vanwelde, C. Carli, and K. Skoufaris, "Progress on the 10 TeV center-of-mass energy muon collider", in *Proc. IPAC'25*, Taipei, Taiwan, pp. 362–365, Nov. 2025. doi:10.18429/JACoW-IPAC2025-MOPM029

[8] D. Schulte, F. Meloni, C. Rogers, and R. Taylor, "Status of the baseline design for a 10 TeV muon collider", in *Proc. IPAC'25*, Taipei, Taiwan, pp. 36–41, Nov. 2025. doi:10.18429/JACoW-IPAC2025-MOZD2

[9] C. Rogers *et al.*, "Preliminary report on key WP4 subsystems", Nov. 2025. doi:10.5281/zenodo.17733000

[10] B. Stechauner, "Final cooling lattice design", Private communication, 2025,

[11] D. Stratakis and R. B. Palmer, "Rectilinear six-dimensional ionization cooling channel for a muon collider: a theoretical and numerical study", *Phys. Rev. Spec. Top. Accel. Beams*, vol. 18, no. 3, 2015. doi:10.1103/physrevstab.18.031003

[12] R. Taylor *et al.*, "MuCol Milestone Report No. 7: Consolidated Parameters", CERN and Muon Collider Collaboration, Oct. 2025. doi:10.5281/zenodo.17476875

[13] R. Zhu, C. Rogers, J. Yang, H. Zhao, C. Guo, and J. Li, "Performance and tolerance study of the rectilinear cooling channel for a muon collider", 2024, arXiv: 2409.02613 [physics.acc-ph],

[14] B. Stechauner, "Investigations and technology developments for a novel muon collider cooling scheme", Ph.D. thesis, 2025. doi:10.34726/HSS.2025.105696

[15] C. Accettura *et al.*, "Mechanical design of a rebco non/metal-insulated 40 t solenoid for the muon collider", *IEEE Transactions on Applied Superconductivity*, vol. 35, no. 5, pp. 1–5, 2025. doi:10.1109/TASC.2024.3504472

[16] C. Accettura *et al.*, "The Muon Collider, Supplementary report to the European Strategy for Particle Physics - 2026 update". doi:10.48550/arXiv.2504.21417

[17] A. Lechner *et al.*, "Radiation shielding studies for superconducting magnets in multi-TeV muon colliders", in *Proc. IPAC'24*, Nashville, TN, USA, May 2024, pp. 2536–2539. doi:10.18429/JACoW-IPAC2024-WEPR26

[18] D. Novelli *et al.*, "Updated magnet limitations for the collider ring", 2024, https://indico.cern.ch/event/1410212,

[19] M. Vanwelde, "Parametric IR optics studies for key parameters", 2025, https://indico.cern.ch/event/1582749/,